Cerebral Cortex Advance Access published September 17, 2010

Cerebral Cortex
doi:10.1093/cercor/bhq163

FEATURE ARTICLE
Cortical Auditory Adaptation in the Awake Rat and the Role of Potassium Currents

Juan M. Abolafia[1], R. Vergara[1,2,3], M. M. Arnold[1,2], R. Reig[1] and M. V. Sanchez-Vives[1,4]

[1]Systems Neuroscience, IDIBAPS (Institut d'Investigacions Biomèdiques August Pi i Sunyer), 08036 Barcelona, Spain, [2]Instituto de Neurociencias de Alicante, Universidad Miguel Hernández-Consejo Superior de Investigaciones Científicas, 03550 San Juan de Alicante, Spain, [3]LAPSo (Laboratorio de Acústica y Percepción Sonora), Universidad Nacional de Quilmes, B1876BXD Buenos Aires, Argentina and [4]ICREA (Institució Catalana de Recerca i Estudis Avançats), 08010 Barcelona, Spain

Juan M. Abolafia, R. Vergara and M. M. Arnold have contributed equally to this work.

Address correspondence to Maria V. Sanchez-Vives, IDIBAPS (Institut d'Investigacions Biomèdiques August Pi i Sunyer), Villarroel 170, 08036 Barcelona, Spain. Email: msanche3@clinic.ub.es.

Responses to sound in the auditory cortex are influenced by the preceding history of firing. We studied the time course of auditory adaptation in primary auditory cortex (A1) from awake, freely moving rats. Two identical stimuli were delivered with different intervals ranging from 50 ms to 8 s. Single neuron recordings in the awake animal revealed that the response to a sound is influenced by sounds delivered even several seconds earlier, the second one usually yielding a weaker response. To understand the role of neuronal intrinsic properties in this phenomenon, we obtained intracellular recordings from rat A1 neurons in vitro and mimicked the same protocols of adaptation carried out in awake animals by means of depolarizing pulses of identical duration and intervals. The intensity of the pulses was adjusted such that the first pulse would evoke a similar number of spikes as its equivalent in vivo. A1 neurons in vitro adapted with a similar time course but less than in awake animals. At least two potassium currents participated in the in vitro adaptation: a Na^+-dependent K^+ current and an apamin-sensitive K^+ current. Our results suggest that potassium currents underlie at least part of cortical auditory adaptation during the awake state.

Keywords: auditory circuits, auditory cortex, auditory processing, cortical slices, forward masking, forward suppression, intrinsic properties, in vitro cortex, potassium channels, sensory adaptation

Introduction

Adaptation to repetitive stimulation is a common feature in sensory systems. Adaptation to known stimuli increases sensitivity toward new ones, acting as a gain control mechanism and influencing stimuli perception. Responses to sound in A1 are known to be affected by the preceding history of stimulation. Stimulus-specific adaptation has been described in the auditory cortex of the anesthetized animal (Brosch and Schreiner 1997; Ulanovsky et al. 2003, 2004; Pienkowski and Eggermont 2009). There the term "specific" is used in the sense that the cortex stops responding to repeated stimuli but remains responsive to rare infrequent sounds. However, not all adaptation is specific to the preceding stimulus (Bartlett and Wang 2005).

Although adaptation was believed to be mostly cortical, it has been recently shown that auditory adaptation also exists in the inferior colliculus (Perez-Gonzalez et al. 2005) and in the auditory thalamus (Anderson et al. 2009; Malmierca et al. 2009). Some of the adaptation observed in the cortex may be transmitted from lower nuclei, and conversely, part of the adaptation observed in those areas may be of descending cortical origin.

A number of different mechanisms that could underlie cortical adaptation (hereby considered as the decreased response amplitude to a second with respect to a first stimulus) have been previously considered: synaptic depression (Wehr and Zador 2005), decreased excitation or lateral inhibition (Qin and Sato 2004), increased inhibition (Zhang et al. 2003), or excitatory–inhibitory imbalance (De Ribaupierre et al. 1972a; Volkov and Galazjuk 1991; Ojima and Murakami 2002; Oswald et al. 2006). Each of these mechanisms involves a network of interneuronal connections. Until now, the role of ionic currents on auditory adaptation has been largely ignored. One of the reasons is that the currents that usually underlie adaptation processes, namely K^+ currents, have not been characterized in the auditory cortex. Potassium currents have been thoroughly studied in other cortical areas, their activation is often activity-dependent, and they can maintain neurons hyperpolarized ranging from tens of milliseconds to tens of seconds (for reviews, see Schwindt, Spain, Foehring, Stafstrom, et al. 1988; Sah 1996; Vergara et al. 1998; Bhattacharjee and Kaczmarek 2005). Potassium channels play a role in sensory adaptation in other sensory areas (Schwindt, Spain, Foehring, Chubb, and Crill 1988; Sanchez-Vives et al. 2000a; Diaz-Quesada and Maravall 2008; Kuznetsova et al. 2008). Depolarization and high frequency firing during sensory responses induce an intracellular increase of ions such as Ca^{2+} or Na^+ that activate ion-dependent K^+ channels and also membrane depolarization can directly activate voltage-dependent K^+ channels. The activation of potassium currents hyperpolarizes the membrane potential and decreases neuronal responsiveness to subsequent inputs. This can happen even in the absence of spikes, via ions entering the cell through α-amino-3-hydroxy-5-methyl-4-isoxazole propionic acid (AMPA) receptors (Nanou et al. 2008).

The above-mentioned studies and some other recent ones (Hildebrandt et al. 2009; Sakai et al. 2009; Szymanski et al. 2009; von der Behrens et al. 2009) have improved insight into the cortical versus subcortical nature of neuronal adaptation, the dependence of neural adaptation on anesthesia, and differences on adaptation between animal species, sound stimulation, and cortical layers. The contribution of intrinsic mechanisms to auditory cortical adaptation remains, however, an open question. In this study, we aimed at exploring the time course of auditory adaptation at the single unit level in the primary auditory cortex (A1) of the freely moving rat. Additionally, we were interested in finding out to what extent auditory adaptation could be supported by the activation of

hyperpolarizing currents. To accomplish this, we mimicked the protocols performed in the awake animals in rat A1 in vitro.

Materials and Methods

Recordings from Chronically Implanted Freely Moving Animals

Recordings were obtained from 6 Lister Hooded rats (300–450 g) chronically implanted with tetrodes in the primary auditory cortex (Doron et al. 2002).

Surgical Procedure

Anesthesia was induced using intraperitoneal injections of ketamine (80 mg/kg) and xylazine (10 mg/kg). The animal was then mounted in a stereotaxic apparatus, and the skull was exposed. During the surgery, the animal was deeply anesthetized using a mixture of isoflurane (0.5–1.2%) and oxygen (1.5 L/min). A trephine was used to make a 3-mm diameter craniotomy over somatosensory cortex (S2) between −3.6 and −5.2 mm A-P and 6.6–7 mm M-L (Paxinos and Watson 1998). These coordinates were used in order to position the microdrive dorsally, which made it more stable than entering laterally right over A1. Body temperature was monitored through a rectal thermometer and maintained (36–38°) by means of an electric blanket. Heart rate and blood oxygen levels were monitored. Reflexes were regularly checked during surgery to assure deep anesthesia. Other drugs were given during surgery and the recovery period in order to prevent infection, inflammation, and for analgesia: antibiotics (enrofloxacin; 10 mg/kg; subcutaneous [s.c.]) and topical application of neomycin and bacitracin in powder (Cicatrin), analgesic (buprenorphine; 0.05 mg/kg; s.c.), anti-inflamatory (methylprednisolone; 1 mg/kg; intraperitoneally) and atropine (0.05 mg/kg, s.c.) to prevent secretions during surgery. Rats were cared for and treated in accordance with the Spanish regulatory laws (Boletin Oficial del Estado 256; 25 October 1990), which comply with the European Union guidelines on protection of vertebrates used for experimentation (Strasbourg; 18 March 1986).

Tetrodes and Microdrives

Each tetrode was made from 4 twisted strands of HM-L-coated 90% platinum-10% iridium wire of 17 and 25 μm diameters (California Fine Wire). If the wire used was 17 μm diameter, gold plating decreased their impedance to ~300 KΩ. Four tetrodes were held by a cannula that was attached to a microdrive supplied by Axona Ltd. This microdrive allowed for dorsal to ventral movement of the tetrodes to search for new units. Microdrives were attached to the skull with dental cement and 7 stainless steel screws. The auditory cortex was reached by vertical descent, and the tetrodes were lowered 100 μm during the surgery. Vertical descent performed after surgery was of 50–75 μm per day until an auditory response was observed. All the recordings included in this study corresponded to A1 (Doron et al. 2002). This estimation is based on the depth of the included recordings and on the anatomical reconstructions of the electrode track. The auditory latencies were 10–20 ms, which are as well characteristic of A1 (Ojima and Murakami 2002; Malmierca 2003; Nelken et al. 2003).

Electrophysiological Recordings

Animals lived in large cages of 70 × 45 × 31 cm (Rody Cavia; SAVIC) in a rich environment, under a 12:12 h light:dark cycle, water, and food ad libitum. After a week of postoperative recovery period, animals were habituated to the recording chamber. The electrode wires were AC-coupled to unity gain buffer amplifiers. Lightweight hearing aid wires (2–3 m) connected these to a preamplifier (gain of 1000) and then to the filters and amplifiers of the recording system (Axona). Signals were amplified (×15 000–40 000), high-pass filtered (360 Hz), and acquired using software from Axona Ltd. Each channel was continuously monitored at a sampling rate of 48 kHz, and action potentials were stored as 48 points per channel (1 ms; 200 μs prethreshold; 800 μs postthreshold) whenever the signal from any of the prespecified recording channels exceeded a given threshold set by the experimenter for subsequent off-line spike sorting (OFS) analysis. Before every experimental session, tetrodes were screened for neuronal activity. Once spikes could be well isolated from background noise the experimental protocol started.

Experimental Set Up

The loudspeaker was located 53 cm above the bottom of the recording chamber. The box was built in black acrylic and had a surface of 22 by 27 cm and the walls had a height of 65 cm. The walls of the box were covered with corrugated cardboard (4 mm thickness) for sound-resonance suppression. Measurements were taken of the sound from different points of the recording chamber, and no differences in the intensity of the sound were detected. During the recordings, the rat was freely moving within the limited space of the chamber. Recordings were obtained in darkness, and the experiment was filmed with an infrared camera placed above the recording chamber.

Presentation of Sound Stimuli

Protocols of stimulation were controlled through Matlab and a National Instrument card and breakout box (FS 300 kHz). Sound triggers had microsecond precision. A WAV-file containing white noise was generated. We first observed the effect of the interstimulus interval on subsequent responses. The sound stimuli had a duration of 50 ms and an intensity of 80–90 dB, being identical for both the first and second stimulus. Pairs of same intensity white noise stimuli were separated by different interstimulus intervals randomly presented and ranging between 50 ms and 8 s (generally 0.05, 0.1, 0.3, 0.5, 0.75, 2, 5, and 8 s). Intertrial intervals varied randomly between 8 and 15 s before the beginning of a new trial. In order to obtain reliable values in the adaptation curve, one complete session of 50–100 trials was carried out for each of the intervals. Animals were continuously recorded for sessions of up to 2 h. The time course of adaptation recovery was fitted by a logistic function. For display purposes, we use a logarithmic scale that expands the early part of the recovery time course.

Once the dependence of auditory responses with respect to the time elapsed since the previous stimuli was studied, we explored to what extent auditory responses varied depending on the intensity or the duration of the preceding stimuli. With that purpose, durations and intensities of the first stimulus were randomly varied between 0.05 and 0.7 s and 70 to 103 dB, respectively.

Spike Analysis

Cluster cutting (isolating single units from the multiunit recording data) was performed using an OFS (Plexon) (Supplementary Fig. S1). Waveforms were first sorted into units by using the valley-seeking algorithm (Koontz and Fukunaga 1972). Waveforms were considered to have been generated by a single neuron when they occurred simultaneously in the 4 electrodes that defined a discrete cluster in 3D principal component (or peak to peak) space distinct from clusters for other units using a multivariate analysis of variance test. Single units exhibited a recognizable refractory period (>1 ms) in their ISI histograms and had a characteristic and distinct waveform shape and peak-to-peak amplitude when compared with other spikes. Single-unit spike analysis consisted of peristimulus histograms (PSTH) and rasters around the time of occurrence of the sensory stimulation.

Recordings from In Vitro Cortical Slices from Rat Auditory Cortex

Slice Preparation

The methods for preparing cortical slices were similar to those described previously (Descalzo et al. 2005). Briefly, rat cortical slices were prepared from 250 g rats that were deeply anesthetized with sodium pentobarbital (40 mg/kg) and decapitated. Four hundred-micrometer-thick coronal slices of the auditory cortex (−3.5 to 5.5 mm) (Paxinos and Watson 1998) were obtained. A modification of the technique developed by Aghajanian and Rasmussen (1989) was used to increase tissue viability. After preparation, slices were placed in an interface-style recording chamber (Fine Sciences Tools) and bathed in artificial cerebrospinal fluid containing (in mM): NaCl, 124; KCl, 2.5; $MgSO_4$, 2; $NaHPO_4$, 1.25; $CaCl_2$, 2; $NaHCO_3$, 26; and dextrose, 10 and were aerated with 95% O_2, 5% CO_2 to a final pH of 7.4. Bath temperature was maintained at 34–35 °C.

Recordings and Stimulation

Sharp intracellular recording electrodes were formed on a Sutter Instruments P-97 micropipette puller from medium-walled glass and beveled to final resistances of 50–100 MΩ. Micropipettes were filled with 2 M potassium acetate. Recordings were digitized, acquired, and analyzed using a data acquisition interface and software from Cambridge Electronic Design. In order to induce a discharge pattern similar to that evoked in the awake animal by auditory stimulation, depolarizing current pulses of the same duration (50 ms) were given. The intensity of the current injection (0.4–1 nA) was adjusted in order to obtain a spike discharge similar to that evoked in the awake animal with 50 ms of white noise and 90 dB, a train of 3–5 action potentials. Pairs of stimuli were separated by intervals between 40 ms and 5 s.

Analysis of Spike Frequency Adaptation

In the awake preparation, a Peristimulus histograms (PSTH) and rasters were generated and the peak value of the response was taken for a 10 ms bin. This method could not be applied in vitro because, given the absence of synaptic noise, the spikes evoked by the same pulse always occurred at the same time. The method then used was to measure the exact time that pulses 1 and 2 took to generate the same number of spikes, most often 2–3 spikes. The measure was similar to the one used to calculate frequency in McCormick et al. (1985). Given that both measures (in vivo / in vitro) refer to frequency (Spikes/s) and both are relative responses (Response2/Response1), they can be compared. In the intracellular recordings, R2/R1 was (Spikes/time R2) / (Spikes/time R1). Since the number of spikes considered was the same (see above) Time 1 / Time 2 was measured. In the extracellular recordings R2/R1 was also (Spikes/time R2) / (Spikes/time R1). Here the time was the same (10 ms per bin) and thus adaptation was measured as Spikes R2 / Spikes R1.

Intrinsically bursty neurons (8 of the in vitro sample) were not included in the analysis of adaptation because the method to calculate their adaptation should have been different and thus not comparable with the rest of the sample. We opted for a more homogeneous sample that only included regular spiking neurons.

Results

Recordings from 76 isolated neurons were obtained in the primary auditory cortex of awake freely moving rats. Among these, detectable auditory responses were evoked in 54 neurons that are included in the study. Similar proportions of responsive neurons have been found by other authors (50% in Hromadka et al. 2008). In addition, recordings from 98 neurons in rat primary auditory cortex in vitro were also included for the second part of the study.

Single Neuron Recordings in A1 from Freely Moving Rats

Single units were identified by means of tetrode recording and subsequent cluster cutting from the freely moving rat (see Materials and Methods). We were concerned to ascertain that the animal was awake during the whole protocol. Experiments were carried out in the dark, where rats have been reported to be awake during 54–66% of the time, around 5% in rapid eye moment (REM) sleep and the rest in non-REM sleep (Bertorelli et al. 1996; Stephenson et al. 2009). Those studies refer to a quiet environment and without sound stimulation, which was not the case here. Indeed, sound has been used before in protocols of sleep deprivation (Franken et al. 1995). In addition, we carried out analysis on the local field potential recordings obtained along with the single units. The analysis followed that described in (Gervasoni et al. 2004). In all analyzed cases ($n = 17$) periods of low frequencies (see Fig. 1*B* in Gervasoni et al. 2004) were rarely observed, while those of theta, normally associated to movement, predominated.

Under these conditions, the mean spontaneous activity was 5.07 ± 3.25 Hz (mean ± standard deviation), ranging between 0.6 and 16 Hz. The distribution of values is illustrated in Supplementary Figure S2A. Mean and standard deviation were similar to reported data from cell-attached recordings in head-fixed animals (Hromadka et al. 2008). The spontaneous frequency was calculated by averaging the firing rate value of each 10 ms bin during a 300 ms time window preceding auditory stimuli (between 50 and 100 trials, 15–30 s intertrial interval). The peak frequency (2 ms bins) of the subsequently evoked auditory responses (50 ms, 80–90 dB) was also measured. A significant positive relationship was found between the spontaneous frequency and the maximum frequency evoked by the stimuli (Supplementary Fig. S2B–E).

Interstimulus Interval and Adaptation

Auditory responses to pairs of 50 ms sounds (white noise) separated by interstimulus intervals spanning between 50 ms and 8 s (from the end of stimulus 1 (S1) to beginning of stimulus 2 (S2); see Materials and Methods) were tested in a total of 30 neurons. After averaging the response to 50–100 trials of stimulation for each interval, we observed that most neurons (83.3%) showed some degree of adaptation in the form of a decreased response to the second identical sound, the adaptation being larger for shorter intervals. The remaining neurons showed either no difference between the two responses (13.3%) or an increased response of the second response with respect to the first (3.4%). Figure 1 illustrates the peristimulus time histogram (PSTH) of the response (spike/s) to 50 trials (bottom) and raster plots (top) in each panel. The responses correspond to the intervals 100, 300, 500, and 2000 ms for one neuron (Fig. 1*A–D*). The response to the second stimulus (R2) was in all cases smaller than the response to the first one (R1). The time course of adaptation is represented for this particular case (Fig. 1*E*). For a 50 ms interstimulus interval, the R2 was 0.35 the peak amplitude of R1. When the interval was increased to 1 s, R2 was on the average 0.80 of R1. In this neuron, a total recovery of the amplitude of R2 with respect to R1 was not completely achieved until an interval of 3 s had elapsed.

The average adaptation time course for 30 neurons is represented in Figure 1*F*. In these cases, for a 1-s interval between the 2 auditory stimuli, R2 had approximately 0.80 the amplitude of R1 and was completely recovered for intervals between 2 and 5 s. We conclude that stimuli occurring 1 or more seconds earlier have an influence on the amplitude of subsequent responses.

Duration of the First Stimulus and Adaptation

In 21 neurons recorded in A1 of the awake rat, the duration of the first auditory stimulus was randomly varied (50, 300, 500, and 700 ms), while the duration of the second stimulus (50 ms) was maintained (Fig. 2*A–C*). The objective was to determine to what extent the adaptation of R2 was contingent on the duration of R1. This was tested for intervals of 300, 400, 500, 750 and 1500 ms between R1 and R2. In 62% of the observations we found an effect of S1 duration, the longer duration of the first stimulus further decreasing R2. In the remaining cases adaptation either remained the same (19%) or there was less adaptation than for shorter stimuli (19%).

Intensity of the First Stimulus and Adaptation

The influence of the intensity of the first stimulus (70–103 dB) in the response to S2 was also explored in 21 neurons for

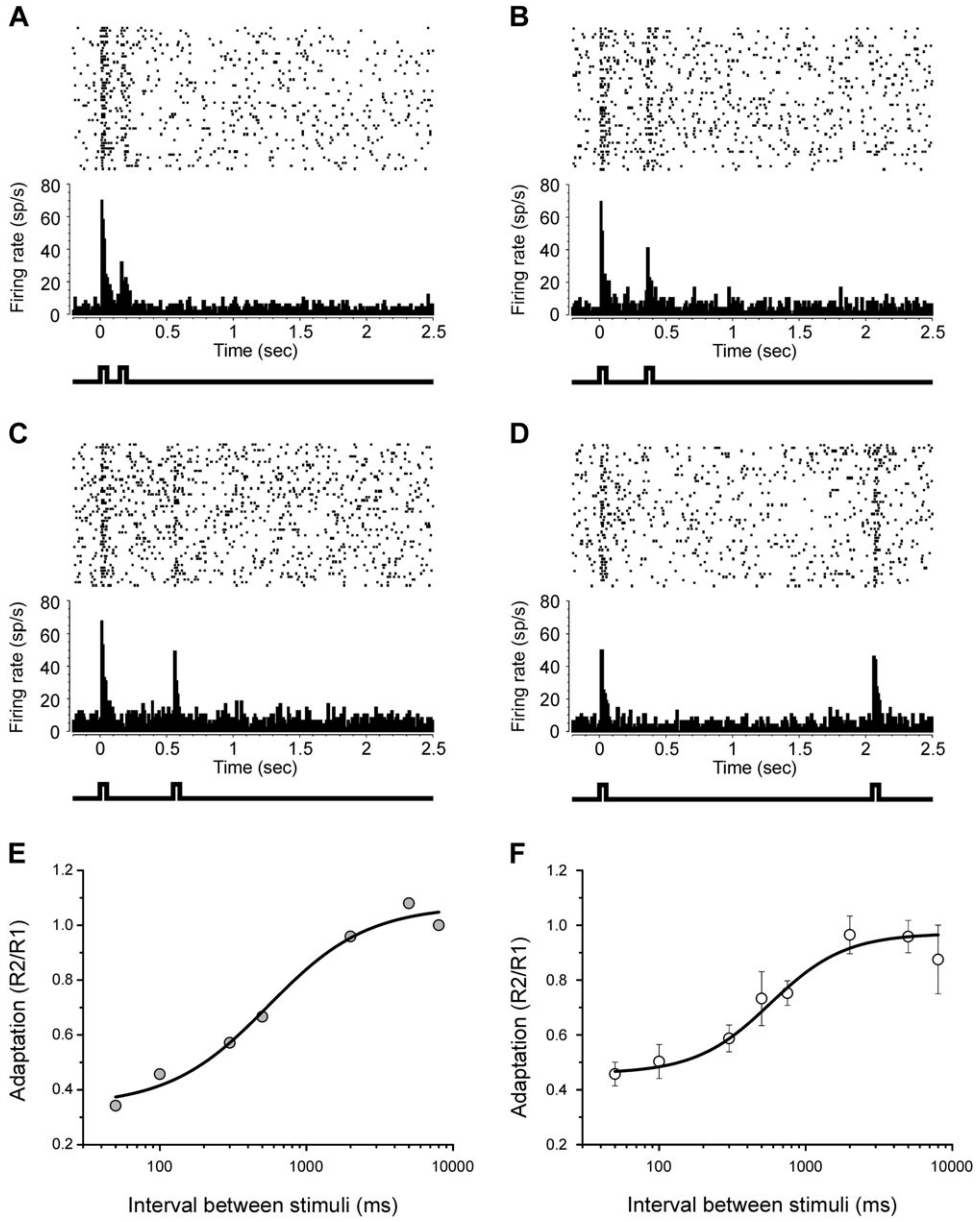

Figure 1. Auditory adaptation in single neuron recordings from A1 neurons in the awake freely moving rat. (*A–D*) Responses to 2 identical sounds (50 ms; 90 dB; white noise) separated by 100, 300, 500, 2000, ms intervals (*A*, *B*, *C*, *D*, respectively). PSTHs of the response (spike/s) to 50 trials (bottom) and raster plots (top) in each panel. (*E*) Relative amplitudes of the peak responses to the second with respect to the first stimulus illustrating the time course of adaptation. The neuron is the same as in panels (*A–D*). A sigmoid was fitted and $R^2 = 0.98$. (*F*) Plot of the relative amplitude of the response to the second sound with respect to the first one for different intervals for an average of 30 neurons. $R^2 = 0.99$. Error bars are SEM. Note that in average 2 s are needed for the second response to have an amplitude which is the same as the first one.

various intervals (50, 100, 200, 300, 400, 500, 750, 1000, and 1500 ms). The intensity of S1 was varied randomly (see Materials and Methods). In 50% of neurons an influence of the intensity of S1 was observed on R2, such that higher intensity of S1 induced stronger adaptation (Fig. 2*D–F*). Of the remaining neurons, the adaptation of 40% remained constant independently from S1 intensity. Finally, the remaining 10% of neurons showed less adaptation for higher than for lower intensities of S1.

Latency of Auditory Responses and Adaptation

As reported by others (Eggermont 1999), the occurrence of adaptation often not only affects the magnitude of responses but also their timing. Here, the timing of responses was first quantified at the response's threshold. The mean firing frequency and the 95% of the confidence interval during the 300 ms preceding the stimulation were calculated. The response to multiple trials (80–100) was represented in a PSTH in 2 ms bins. After 10 ms of stimulus presentation, the first bin that crossed the 95% confidence interval was taken as the onset of the auditory response, and the exact time taken was the mid value of a 2 ms bin (Supplementary Fig. S3).

Auditory responses following the shortest interstimulus intervals (<0.3 s) often did not cross the 95% confidence interval and thus their latency could not be determined. In order to detect possible changes in latency with adaptation, interstimulus intervals were classified into short ISIs (0.05, 0.1, 0.3, 0.4, and 0.5 s) and long ISIs (0.75, 2, 5, and 8 s). Auditory

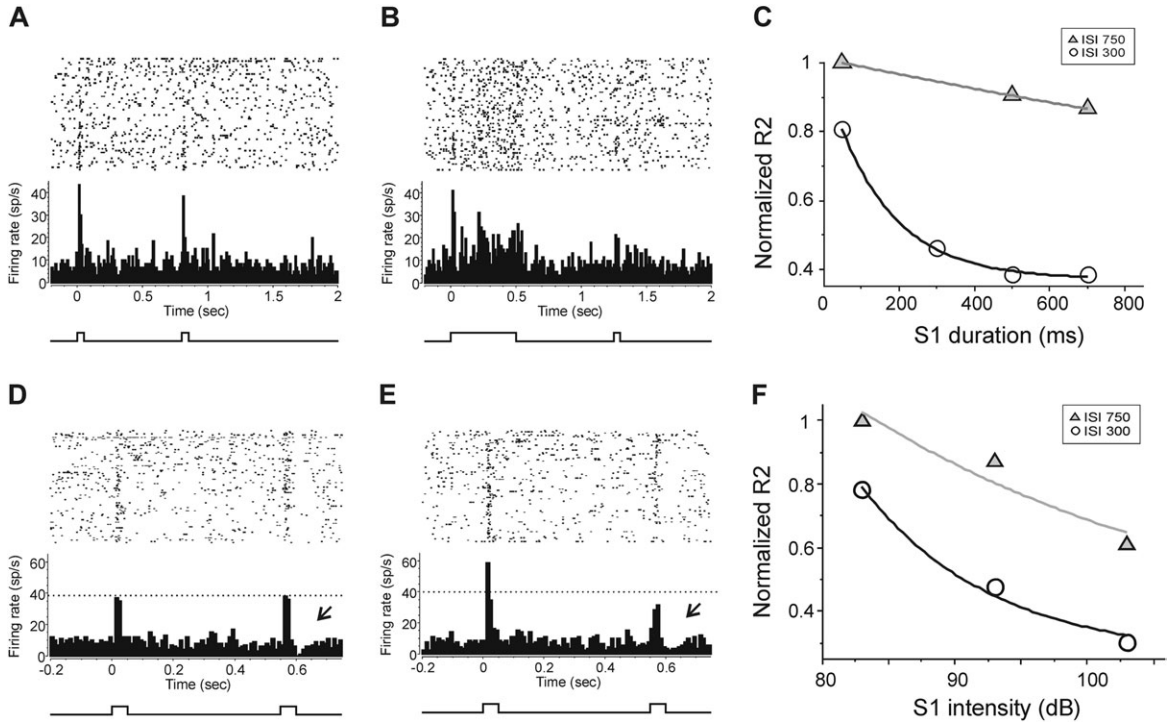

Figure 2. Relative adaptation of the second auditory response with respect to the first one in A1 of the awake rat. (*A*) Plot of the PSTH for one A1 cell to 60 trials of two 50 ms white noise sounds (90 dB) presented at 750-ms interval. On top, raster plots. (*B*) PSTH shows a decrease of the response to the second sound when the duration of the first is prolonged up to 500 ms. (*C*) Normalized response to the second sound (R2; 50 ms) (R2 divided by the value of the maximum R2, which occurs when the duration of S1 equals that of S2) represented against the duration of the first one for 2 intervals (300 and 750 ms). (*D*) Plot of the PSTH for one A1 cell to 100 trials of two 50 ms white noise sounds (90 dB) presented with 500-ms interval. (*E*) PSTH of the responses to both stimuli when the intensity of the first stimulus has been increased to 100 dB. Note that the response R1 increases, while R2 decreases. An arrow points to the postadaptation following the second stimulus (*D*, *E*). (*F*) Normalized response to the second sound (R2) (as in *C*) for different intensities of the first stimulus and for 2 different intervals (300 and 750 ms).

responses following short ISIs had significantly longer delays (12 ± 1 ms) than those following long ISIs (11 ± 2 ms; $n = 26$) ($P < 0.0003$), although the difference was small. It is possible that this difference was underestimated given that the most adapted responses (ISI < 0.3 s) were not included.

Auditory responses to S2 following long duration S1 (500 ms) had also significantly longer response delays (mean: 12 ± 2 ms; $P < 0.003$) than those following shorter stimuli (50 ms, mean: 11 ± 1 ms) ($n = 20$). Latency was also significantly ($P < 0.01$) longer for S2 stimuli following louder S1 stimuli (95 dB) (S1 = 11.9 ms, S2 = 13 ms). Whereas for louder S1 (95 dB), the response's latency was significantly shorter (11 ± 1 ms) than for 70 dB S1 (13 ± 2 ms; $P < 0.023$; $n = 21$) as reported earlier (Polley et al. 2006). For details on statistical analysis of response delays, see Table 1 in Supplementary Material.

The difference in latency was consistent across individual cases, and for that reason it was statistically significant in spite of the small latency difference (around 1 ms). An increased latency of the first evoked spike was also detected in the adapted responses while in vitro (see below). Even when the measure used here has been used by other authors, a decreased response amplitude may result in an artifactual increase of the latency when detected at the response's threshold (Bair et al. 2003). We therefore repeated the latency measures at the peak of the response and at 50% and 25% of the peak. In that case, no significant differences in the latency between the first and the second responses were detected (Supplementary Table S1). To conclude, the consistent but small differences in latency detected at the threshold of the adapted responses were not robust enough to persist when measured at the 25%, 50%, or 100% of the response's peak amplitude.

Postadaptation Following Auditory Responses

We refer to "postadaptation" as the decay in the spontaneous activity firing following the end of an auditory response (Fig. 2*D*,*E*, see arrows). PSTHs (10 ms bins) were generated in order to quantify postadaptation. A 95% confidence interval was determined, and the first bin following the auditory response that was below the 95% confidence interval was considered postadaptation (Supplementary Fig. S4). Postadaptation was detected in 79% of cases following S2 and in 59% of cases following S1 ($n = 26$ neurons).

We observed more postadaptation following S2 when S1 was of longer (≥500 ms) duration (89%) than with short (<500 ms) duration stimuli (70%) (e.g., Supplementary Fig. S4*B*). Finally, we found (Fig. 2*D*,*E*) more postadaptation after S2 when it was preceded by a short ISI (<0.3 s) (71%) than by a longer (>0.3 s) ISI (60%).

Mechanisms of Neuronal Adaptation in Auditory Cortex In Vitro

In order to explore to what extent the process of adaptation could be generated by activation of intrinsic membrane currents, 98 neurons recorded from rat A1 slices were included in the study ($n = 34$ rats). All neurons included were recorded from layers 2/3 and 4 and they were regular spiking. Eight additional neurons classified as intrinsically bursting (Nowak et al. 2003) were not included (see Materials and Methods). The average input resistance was 50.6 MΩ ($n = 89$).

Time Course of Adaptation

In order to evaluate the time course of adaptation of these neurons, a paradigm for neuronal stimulation was used that mimicked the one presented to the awake animal in the form of sounds. The paradigm used in vivo consisted of 2 sounds of 50 ms duration that were separated by different time intervals (ranging from 50 ms to 8 s), and it was replicated in vitro by means of current injection. Thus, pairs of square pulses of 50 ms duration separated by time intervals ranging from 50 ms to 5 s were injected. The intensity of the pulse was adjusted such that the first stimulus would induce a neuronal response of 3–5 action potentials, similarly to the response that a 50 ms sound stimulus evoked in the awake animal (Fig. 1). No spontaneous activity occurred in the slices, either supra or subthreshold, and therefore the observed events could be exclusively attributed to the activation of intrinsic membrane currents and not to activation of synaptic conductance. In addition, 6 of the recordings were performed under local application of 100 μM 6-cyano-7-nitroquinoxaline-2,3-dione, which did not affect adaptation or the subsequent afterhyperpolarization (AHP).

Adaptation defined as a decrease in the action potential frequency evoked by the second pulse with respect to the first pulse was detected in all cases (Fig. 3). The amount of adaptation and the time course of its recovery were evaluated in a total of 36 neurons. The time course of adaptation was averaged for all neurons (Fig. 3*D*). For the intensities used, the response evoked by the second pulse was still diminished with respect to the first one for intervals of 1 s between stimuli, while for intervals of 2 s the response was almost totally recovered. Still, there is a large heterogeneity across neurons. In Figure 3*C*, the normalized values of adaptation for 36 neurons are shown. For the sake of intelligibility of the graph, only the fitted sigmoidal curves have been displayed. In Figure 3*D*, the average adaptation recorded in the awake animal and that in the slices have been overlapped. There we can observe that the adaptation is larger in awake animals than in the slices. Hence, the maximum adaptation that occurred for the 50-ms interval was to 0.46 in awake animals and to 0.70 in the slice.

Duration of the First Stimulus and Adaptation

In 11 neurons, the influence of the duration of the first square pulse on the spike frequency adaptation was explored (Fig. 4*A–C*). The protocols carried out in awake animals by means of sound stimulation were mimicked in vitro by using current injection, and the duration of the first pulse was varied between 100, 200, 300, 500, and 700 ms, while the second pulse was of

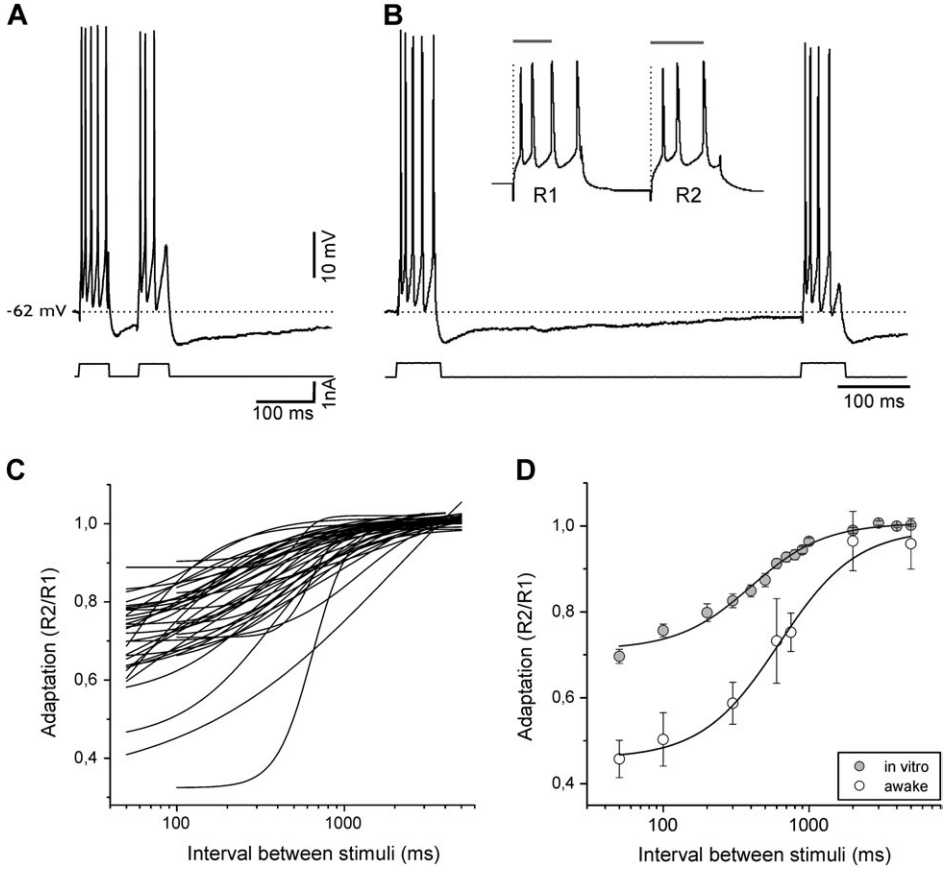

Figure 3. Time course of adaptation in A1 cortical slices and its comparison with adaptation in vivo. (*A*) Intracellular recordings illustrating the injection of two 50 ms pulses of 0.9 nA separated by a 50 ms interval. The intensity was adjusted to evoke 4–5 spikes with the first stimulus to mimic the sound stimulation in vivo. At the bottom trace, the current. (*B*) Recording from the same neuron as in A, but now the interval is 500 ms. The inset illustrates how the spike rate computed as responses (R1, R2) was calculated. It was taken as the time for the same number of spikes to be fired in R1 and R2 (for details see Materials and Methods). The 3 spikes shown in the inset in Figure 3*B* took, from time 0 (represented with a discontinuous line) 28.52 ms and 39.07 ms. (*C*) The recovery from adaptation in 36 neurons is represented, the protocol being that in panels A–B. For the sake of clarity, the sigmoidal fits are represented in order to illustrate the relative heterogeneity across cells and how in most cases adaptation was recovered in 2 s. (*D*) Relative frequency rate of the second response with respect to the first one for different intervals (50 ms–5 s) between identical 50 ms pulses of current injection as in *A* and *B* were averaged for 36 A1 neurons in vitro (gray circles). In order to compare with the adaptation evoked by a similar protocol in vivo, data from in vivo that has been plotted in Figure 1*F* is also displayed. A logistic function has been fitted (see Materials and Methods) and x_0 is 622 ms awake and 400 ms in vitro. In both cases $R^2 > 0.99$. Error bars are SEM.

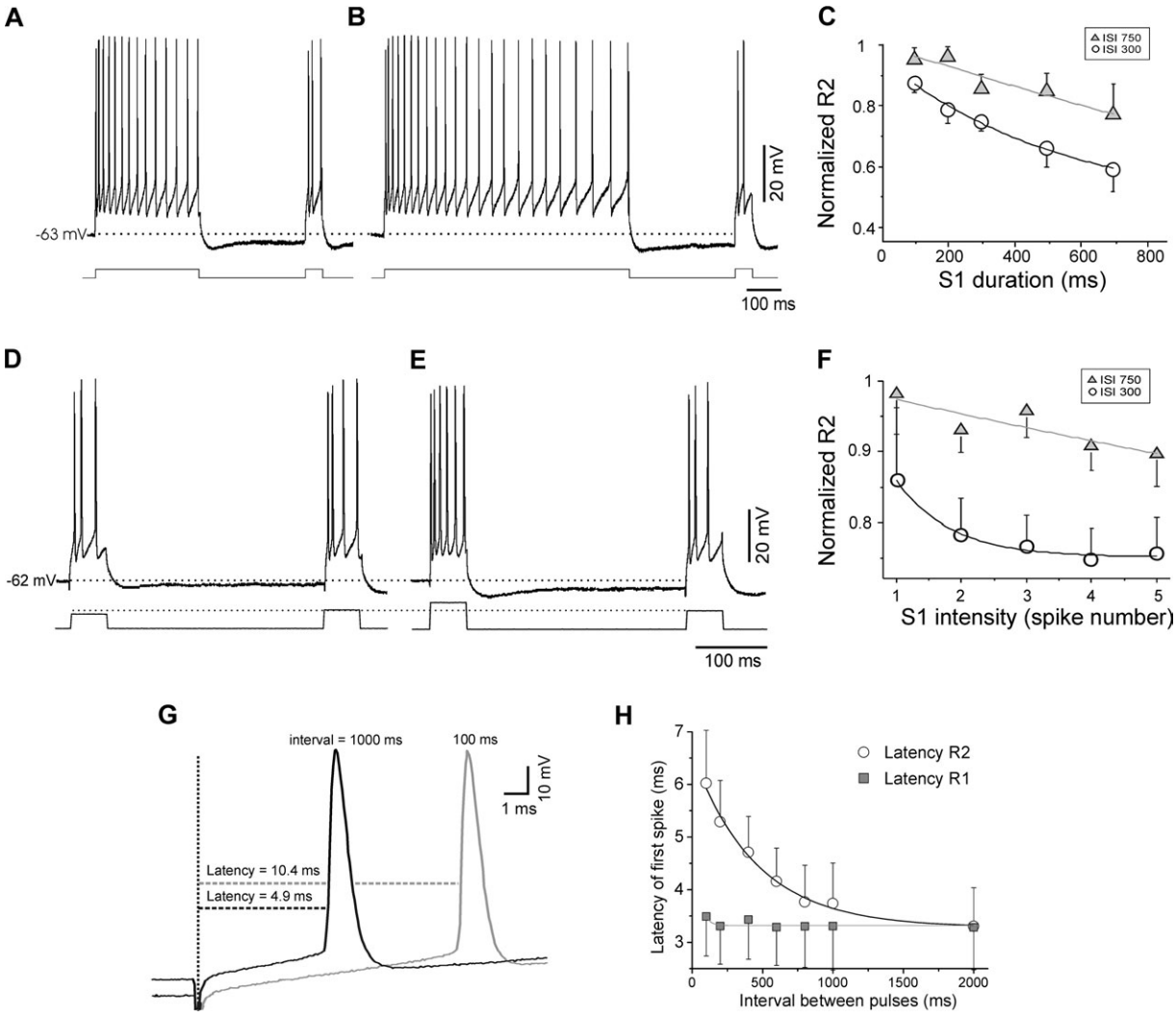

Figure 4. Attenuation of the response to the second pulse depends on the intensity and duration of the first pulse. (*A*) Intracellular recordings of a neuron while the duration of the first stimulus (S1) was varied between 100 and 700 ms. In the panel S1 = 300 ms. S2 was of the same intensity as the first one (0.7 nA) but only 50 ms duration. (*B*) Same recording but here the duration of S1 was 700 ms. (*C*) Average (n=11) normalized response (response to stimulus 2 divided by the response to an identical isolated stimulus, which has the maximum evoked response amplitude) is represented for different durations of S1. Normalized exponential fits at two different intervals (750 and 300 ms) show that response to S2 decreased when S1 was longer. (*D*),(*E*) Intracellular recordings of the responses to two 50 ms pulses while the intensity of the first pulse is varied between 0.4 nA (*D*) and 1.5 nA (*E*). The intensity of S1 affected R2 response. (*F*) Average ($n = 14$) normalized response 2 (as in *C*) (for different intensities of S1 and two intervals (300 and 750 ms). (*G*) First spike latency for S2 separated from S1 by 1000 ms (4.9 ms) and 100 ms (10.4 ms). (*H*) Average (n = 7) latency of first spike (ms) represented against the interval between pulses (50 to 2000 ms).

50-ms duration (Fig. 4*A*,*B*). As in vivo, 2 intervals between the stimuli were tested, at 300 and 750 ms. Figure 4*C* represents the average adaptation for both intervals. When compared with the one in the awake (Fig. 2*C*), we see that the adaptation detected when the interval between pulses is 750 ms was similar in both cases. However, for shorter intervals (300 ms), the adaptation was larger in the neurons of awake animals.

Intensity of the First Stimulus and Adaptation

In 14 neurons, we explored the influence of the intensity of the first pulse on the spike frequency adaptation to the second pulse (Fig. 4*D*–*F*). The maximum number of spikes evoked with a 50 ms pulse in regular spiking neurons was usually 4–5. The intensity of the first pulse was adjusted in order to evoke a number of spikes between 1 and 5 (usually between 0.4 and 1.3 nA). The intensity of the second pulse was constant and adjusted in each cell to evoke 4 spikes (0.4–0.8 nA). Figure 4*F* represents the average adaptation ($n = 14$) for 2 different intervals between the pulses, 300 and 750 ms, which again is less to the one evoked by a similar protocol in the awake animal (Fig. 2*F*).

Latencies of the Spike Response

Not only does the amplitude of the spike response vary but also the latencies of the spikes evoked by the second pulse varied with the time interval since occurrence of the first pulse (Fig. 4*G*). Figure 4*H* illustrates how the average latency remained constant for the response to the first pulse R1 around 3.3 ms, increasing to 6 ms for 100 ms intervals and then decaying progressively for longer intervals all the way to 3.3 ms.

Intrinsic properties may thus account for the increased delay that we observed as well as the one reported by others both in the anesthetized (Brosch and Schreiner 1997; Kilgard and Merzenich 1999; Chimoto et al. 2002; Ter-Mikaelian et al. 2007)

and the awake animal (Brosch and Schreiner 1997; Kilgard and Merzenich 1999; Ter-Mikaelian et al. 2007).

Spike Frequency Adaptation and AHP

In order to understand the basis of the spike frequency adaptation in the A1 cortical neurons in vitro, we explored the underlying mechanisms. An AHP followed the spike trains in all cases (Fig. 3*A,B*). The average AHP following a 50 ms pulse that evoked 4–5 action potentials (the average "first pulse" during the protocol) had a mean amplitude of 6.5 ± 0.4 mV when measured from a membrane potential of –60 ± 2 mV, and a mean duration of 1678.2 ± 107.1 ms (n = 36; x ± standard error of the mean [SEM]) (Fig. 3*A,B*). The amplitude and duration of the AHP increased with the number of spikes (Fig. 5*A*) up to a plateau (Fig. 5*D,E*). During the AHP, there was a decrease in the excitability of the neuron. Figure 5*C* illustrates the silencing of a neuron's tonic firing for 700 ms coinciding with the AHP that follows a 100 ms spike train. When the amplitude of the AHP was measured at different times (between 50 ms and 5 s) following a 50 ms depolarizing pulse, the repolarization from the AHP followed a very similar time course to the recovery of spike frequency adaptation (Fig. 5*B*). This is very suggestive of a relationship between the AHP following the first pulse and the spike frequency adaptation during the second pulse. The significant correlation between AHP duration and adaptation in the population (for 50 and 500 ms intervals) is illustrated in Supplementary Figure S5.

To explore the ionic basis of the AHP, two K^+ currents that for their time courses could be involved in the process were studied: apamin-sensitive Ca^{2+}-dependent K^+ current (Pennefather et al. 1985) and Na^+-dependent K^+ current (Schwindt et al. 1989). These two currents have been found to influence the time course of neuronal responses in the cat (Schwindt et al. 1988).

The application of apamin (500 nM; local application) partially blocked the AHP following a 50 ms depolarizing pulse and spike train (Fig. 6*A,B*). The partial blockade was measured as the reduction of the AHP peak amplitude, which occurred in all cases (n = 20; Fig. 6*C*, inset) and consisted of an average decrease of the peak to 62% of the amplitude. Not only was the AHP partially blocked by apamin but the adaptation of the response to the second stimulus was also consistently reduced (Fig. 6*C*; n = 20). For each of the 20 cells, the pairs of pulses separated by different intervals were given at the same membrane potential before and after the application of apamin. Adaptation was less in the presence of apamin, especially for those pulses separated by the shortest intervals (50 and 100 ms). This finding supports that apamin-sensitive Ca^{2+}-dependent K^+ current underlies at least the earlier adaptation (<200 ms) following a 50 ms spike discharge.

Apamin did not block the slower part of the AHP (Fig. 6*B*). We next explored to what extent Na^+-dependent K^+ current, a current of a slower time course (Schwindt et al. 1989) was playing a role on spike frequency adaptation in A1. To this end, [Na^+] was reduced from 152 to 26–42 mM by replacing NaCl with choline chloride in the bath. To prevent the action of choline on muscarinic receptors, we include the muscarinic antagonist scopolamine (10 μM) in the bath. Scopolamine per se does not have a direct effect on the AHP (Uchimura et al. 1990; Sanchez-Vives et al. 2000a), and this is in agreement with what we observed here. In these conditions, the size and duration of the AHP were significantly reduced (n = 11). Indeed, when [Na^+] was decreased following apamin application, the AHP often was totally blocked (n = 7; Fig. 6*D*). Spike

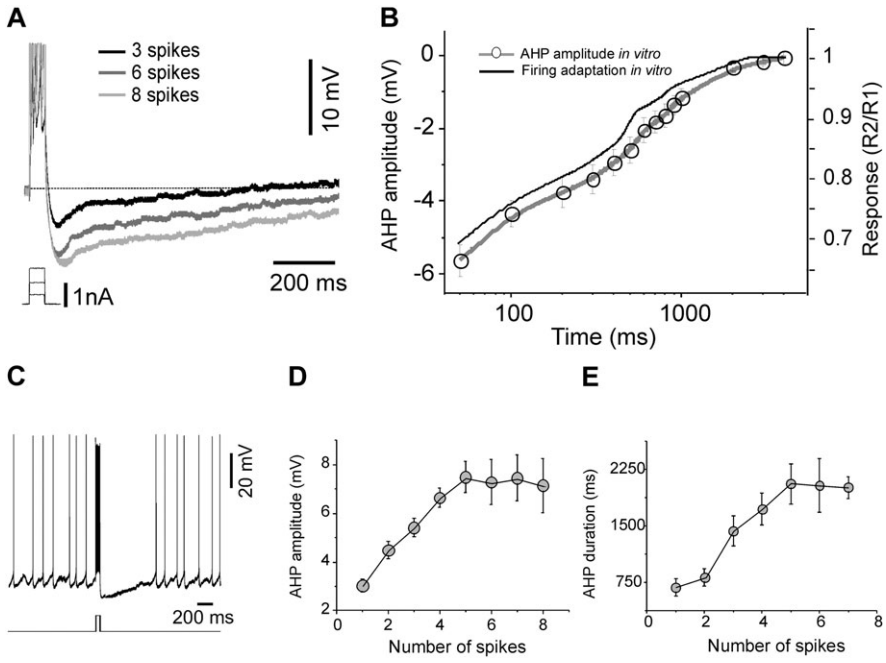

Figure 5. AHP in rat A1 neurons in vitro. (*A*) A suprathreshold 50 ms pulse activates an AHP that increases with the number of action potentials. Pulses of 0.5, 1, and 1.5 nA evoked 3, 6, and 8 spikes and were followed by AHPs of 600 ms, 1 s and 1.3 s, respectively. Top trace is Vm, the schematics of the injected current are represented below. (*B*) This graph represents an AHP following a 50 ms pulse, and the attenuation of R2 firing frequency with respect to R1 in the same neuron. (*C*) Intracellular recording during the tonic firing of a cortical neuron (−54 mV). A pulse of 0.9 nA has been given and the subsequent AHP maintains the neuron silent for 700 ms. (*D*) AHP amplitude at the peak increases with the number of spikes evoked by a 50 ms pulse (n = 24). (*E*) AHP duration increases with the number of spikes evoked by a 50 ms pulse (n = 20).

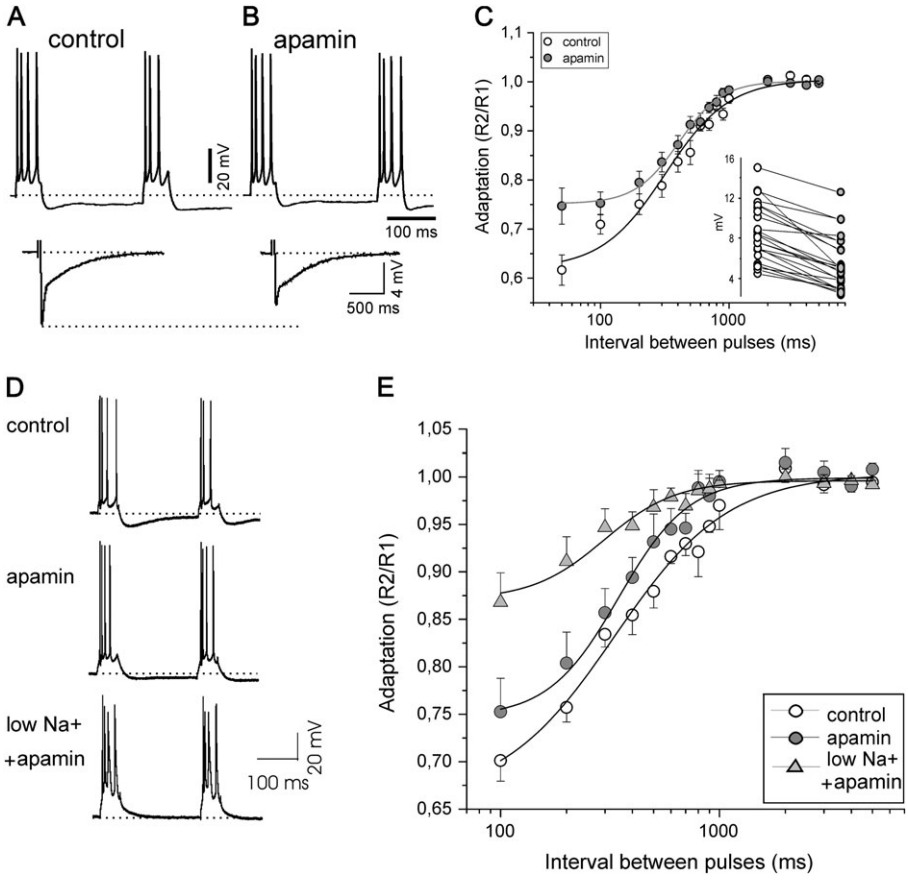

Figure 6. Role of Ca^{2+} and Na^{+} dependent K^{+} channels on adaptation. (*A*) Two 0.9 nA pulses separated by a 200-ms interval evoke 4 and 3 action potentials, respectively. The AHP following the first pulse is displayed below, having an amplitude of 12.7 mV. (*B*) Apamin 1 μM was locally applied. Note that now the second pulse evokes also 4 action potentials as does the first one, plus the AHP amplitude has been reduced to 5 mV. (*C*) Time course of the adaptation recovery in control and in apamin in 20 neurons. Note that adaptation is reduced in apamin, particularly for shorter intervals between pulses. In the inset, the peak amplitude of the AHP in control and in apamin. A logistic function was fitted to the recovery from adaptation (see Materials and Methods). Control, $x_0 = 318$ ms; A2 = 0.62; $R^2 = 0.97$; apamin, $x_0 = 406$ ms; A2 = 0.75; $R^2 = 0.99$; (*D*) Two pulses of 0.9 nA separated by 200 ms in control, apamin, and low sodium plus apamin. (*E*) Time course of the adaptation recovery in control, apamin, and low sodium plus apamin in 7 neurons. Note that adaptation is reduced in apamin and in low sodium. The parameters of the fitted logistic function were: control, $x_0 = 332$ ms; A2 = 0.66; $R^2 = 0.99$; apamin, $x_0 = 354$ ms; A2 = 0.76; $R^2 = 0.95$; low Na^{+}, $x_0 = 296$ ms; A2 = 0.87; $R^2 = 0.92$.

frequency adaptation was again tested with the same protocol as above while in apamin plus low $[Na^{+}]$. In low $[Na^{+}]$, action potentials were still generated, although their amplitude was reduced and their duration increased. This was tested in 7 neurons and the resulting average adaptation has been represented in Figure 6*E*. Lowering $[Na^{+}]$ further blocked the adaptation already reduced by apamin. Still, a certain level of spike frequency adaptation remained, probably partly the result of the remaining Na^{+}-dependent K^{+} current given that $[Na^{+}]$ was not totally eliminated from the bath. Reduction of sodium has a similar effect to replacement with lithium (Franceschetti et al. 2003) and has been used before to study Na^{+}-dependent K^{+} currents (Sanchez-Vives et al. 2000a). Still, the caveat of reducing the size of action potentials is that it may affect the activation of other channels.

Adaptation in Neurons with Background Activity

One of the differences that exist between the awake animal and the slice is that neurons in the slices were silent, while in the awake animal there was ongoing activity. Ongoing firing may have an influence on the intrinsic adaptation itself, setting neurons in a different adaptive state. To explore the effect of ongoing activity on adaptation, spontaneous activity of one neuron in the awake animal was recorded for 20 min in the absence of auditory stimulation (Fig. 7*A*). A period of 10 s was selected, the average firing frequency during this period being 5.5 Hz. At the time of occurrence of each spike, a brief pulse of 2.5–4 ms was injected, adjusting the intensity such that it would evoke just one spike per pulse (2.4–3 nA) (Fig. 7*B*,*C*). This fake "spontaneous" firing also induced the activation of AHPs that would follow action potentials (Fig. 7*D*), and an average membrane potentials that was in average 3.01 ± 1.92 mV ($n = 9$) more hyperpolarized than that in silent neurons. The stimulation (background activity) was looping continuously over which the whole protocol of stimulation was carried out. The same protocols of adaptation used above were repeated, following what was described earlier for silent slices (Fig. 7*E*). The intensity of S1 was adjusted such that the first pulse would evoke 3–5 action potentials. The degree and time course of adaptation were calculated for 9 neurons (Fig. 7*F*). The standard deviation of each of the points (SEM in the error bars) was larger than for the adaptation than in silent slices due to the noise added by the background activity. The adaptation curve and its time course in neurons with background activity

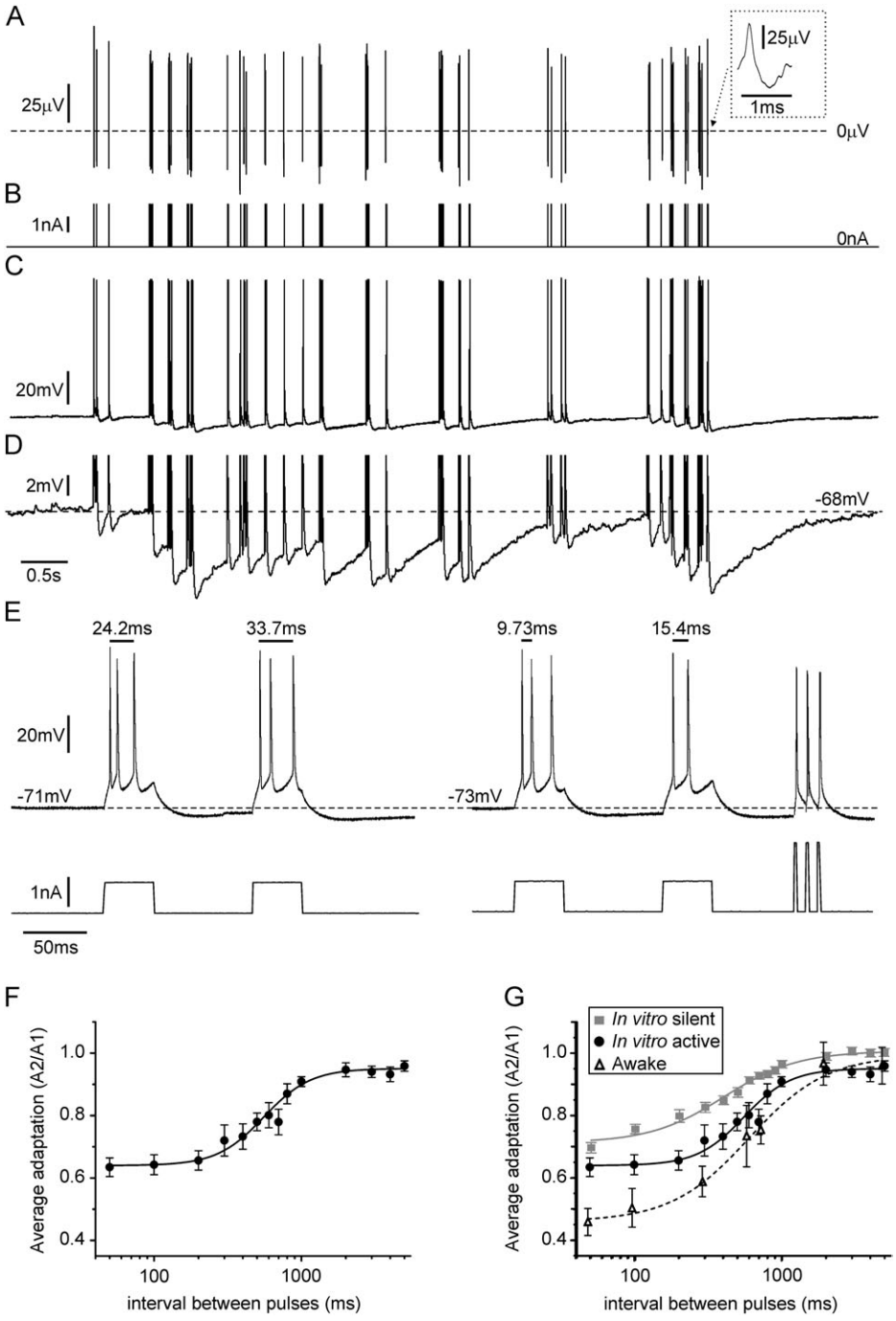

Figure 7. Adaptation R2/R1 in neurons with background activity mimicking the one in the awake animal. (*A*) Raw trace of single spikes recorded in the awake rat. The inset shows an expanded spike. (*B*) Current square pulses (2.5–4 ms) following time pattern of the firing in A. The pulses we reinjected in silent neurons to mimic the firing in the awake animal. (*C*) Intracellularly recorded neuron firing one action potential per injected pulse. (*D*) Expanded trace of intracellular recording shown in (*C*) to illustrate membrane potential changes as well as the increases in AHP in response to spiking activity. The dash line marks the resting Vm while in silence. (*E*) Two raw traces of the intracellular recording (top) to illustrate the neuronal response to two 50 ms square pulses (ISI = 100 ms) (bottom). Left and right trace; neuron without and with "fake" spontaneous firing in response to short pulses, respectively. Note that the Vm is more hyperpolarized in the active neuron and its adaptation is larger. (*F*) Time course of adaptation recovery average in neurons with "fake" spontaneous firing. A logistic function has been fitted (see Materials and Methods, $R^2 = 0.91$, $N = 9$). (*G*) Summary of the average adaptation time course in in vitro silent, in vitro active, and in awake preparations.

(Fig. 7*F*) were then represented along with the average one in the awake state (Fig. 1*F*) and in the silent slice (Fig. 3*D*) in Figure 7*G*. Interestingly, intrinsic adaptation evoked in neurons with "fake" background activity was larger than that in silent neurons (Fig. 7*E*,*G*) and hence closer to that in the awake animal.

Discussion

We have used a combined in vivo (awake) and in vitro approach to study the functional mechanisms that mediate cortical auditory adaptation and with this we have demonstrated that part of the adaptation observed in awake animals

can be explained by the activation of potassium currents. The results reveal auditory adaptation using pairs of auditory stimuli in single neurons in the awake freely moving rats. Heterogeneity across cells with respect to the degree of adaptation and its time course were found, the time courses ranging from hundreds of milliseconds to several seconds. A replica of the stimulation protocol used in the awake animal was reproduced by means of current injection in A1 cortical slices. In this case a possible underlying mechanism of auditory adaptation, so far overlooked, was explored in detail: the participation of K^+ currents.

Auditory Adaptation in the Anesthetized and the Awake Preparations

Studies in anesthetized animals have been relevant for our current understanding of auditory adaptation. However, anesthesia induces changes in neuronal excitability, facilitates oscillatory activity, modifies spontaneous activity, or increases neuronal frequency tuning sharpness (Gaese and Ostwald 2001). The effects vary with different anesthesias, affecting phenomena such as sensory adaptation (Wehr and Zador 2005; Moshitch et al. 2006; Rennaker et al. 2007). Wehr and Zador (2005) showed that pentobarbital anesthesia in the rat prolonged the very slow component of adaptation (several hundreds of milliseconds in that case), while ketamine has been reported to reduce the maximum rate of responses to repeated clicks (Rennaker et al. 2007). Cortical auditory adaptation in anesthetized cats has been described for different anesthesias and protocols displaying a variety of time courses including 50–1600 ms (Hocherman and Gilat 1981), or up to 400 ms (Calford and Semple 1995; Brosch and Schreiner 1997), and even reaching tens of seconds (Ulanovsky et al. 2004; Pienkowski and Eggermont 2009).

Awake animal preparations bypass the problems associated with anesthesia. Additionally, in this study, we have found that the impact of a 50 ms sound on subsequent responses to an identical stimulus persists for several seconds in the awake rat. This effect was normally expressed through attenuation of the response to the second stimulus. Larger responses induced by the first stimulus due to longer or more intense stimuli provoke a larger attenuation of R2 (Fig. 2). Similarly, previous studies found adaptation in the responses to the second sound in a 2-sound sequence for intervals up to 1–2 s in the anesthetized cat (Hocherman and Gilat 1981; Calford and Semple 1995; Brosch and Schreiner 1997; Reale and Brugge 2000) or up to 300 ms in the awake cat (Fitzpatrick et al. 1999). Neuronal adaptation in the passive listening primate was found to last no more than 2 s (Bartlett and Wang 2005), while in the primate performing a task has been reported to last up to 5 s (Werner-Reiss et al. 2006), suggesting that the brain state may have an impact on the duration of adaptation. The fact that cortical adaptation also exists in the awake restrained rat was also observed by Anderson et al. (2006). Using a different conceptual framework, different stimulation paradigms (broadband 80 μs clicks), and a different recording technique (multiunit recordings), Anderson et al. (2006) focused on the detection of the maximum stimulus rate that A1 responses can track (synchronization boundary). In spite of these differences, some of the reported findings in Anderson et al. are in agreement with those presented here, specifically, the decrease in mean response rate and duration with the stimulation rate, as well as the description of postadaptation.

The motivation to characterize auditory adaptation in the awake rat done in this study was first to obtain data on adaptation in freely moving animals, given that most of the previous studies were done in anesthetized preparations. Besides, doing these experiments allowed us to design a specific protocol that we could replicate in the auditory cortex in vitro by means of intracellular current injection in order to study the possible participation of potassium channels on auditory adaptation.

Cellular and Network Mechanisms of Cortical Auditory Adaptation

Different mechanisms that could underlie cortical auditory adaptation have been proposed. Adaptation occurring at lower levels, in the inferior colliculus (Malmierca et al. 2009) or the auditory thalamus (Anderson et al. 2009; Antunes et al. 2010), could contribute to what is observed in the cortex. Still, adaptation appears to be larger in cortical layers that do not receive subcortical input (Szymanski et al. 2009), suggesting that part of it is being generated through the cortical circuitry.

Synaptic depression, both thalamocortical and intracortical, has been proposed as a suitable stimulus-specific mechanism since it can be associated to specific inputs to the neuron (Ulanovsky et al. 2004; Percaccio et al. 2005) and it can provide a variety of time scales (Varela et al. 1997; Carandini et al. 2002). Still, synaptic depression in vivo is less than that in cortical slices, showing an inverse relationship with the occurrence of ongoing activity in the cortical network (Reig et al. 2006). Inhibition could also play a role in auditory adaptation, a mechanism that would provide stimulus specificity (Zhang et al. 2003), as proposed by Eytan et al. (2003) based on ex vivo networks. Intracellular recordings in the cortex of the anesthetized rat (Wehr and Zador 2005) revealed that inhibition plays a role in the adaptation during the first 50–100 ms after the stimulus. However, this does not explain the adaptation of slower time course spanning from 100 ms to tens of seconds, for which $GABA_B$ receptors were proposed by some authors (Buonomano and Merzenich 1998) but found not to be involved by others (Wehr and Zador 2005). AHPs following auditory responses were described already in the first intracellular recordings from this region (De Ribaupierre et al. 1972b), being mostly attributed to IPSPs (De Ribaupierre et al. 1972b; Tan et al. 2004; Wehr and Zador 2005). Our data suggest that at least part of these AHPs may be due to the activation of potassium currents.

Intrinsic Mechanisms and Cortical Adaptation

Most of the studies dealing with adaptation or forward masking/suppression have ruled out intrinsic mechanisms as a possible underpinning mechanism. Hyperpolarizing membrane currents have been found to play an important role in sensory adaptation in other sensory systems (Sanchez-Vives et al. 2000a, 2000b; Diaz-Quesada and Maravall 2008; Kuznetsova et al. 2008). Their activation depends on neuronal depolarization and eventually firing (Nanou et al. 2008), independently of the origin of the depolarization. This lack of dependence on the input is the reason why ionic currents have been largely ruled out as a suitable player in auditory adaptation, which is stimulus–frequency specific (Ulanovsky et al. 2003, 2004; Wehr and Zador 2005).

So, how could K^+ currents support frequency-specific adaptation? First, not all auditory adaptation is stimulus-specific

(Bartlett and Wang 2005). Second, in A1 different frequencies follow a tonotopic map (Doron et al. 2002) and usually neurons in the same electrode track share the same preferred stimulation frequency (Read et al. 2002). Adaptation is very similar in each particular cortical column, with no differentiation according to layers (Ulanovsky et al. 2004 but see Szymanski et al. 2009) but across columns. In a highly interconnected network such as a cortical column, the activation of hyperpolarizing currents in even a small percentage of neurons reverberates in the local circuits, inducing modulation of activity in the whole circuit (Compte et al. 2003). Given the predominance of vertical versus horizontal connectivity, adaptation would not necessarily propagate to adjacent areas of different preferred frequency. In this way, intrinsically mediated adaptation could also become stimulus-specific.

A role for potassium currents in adaptation is compatible with the participation of other mechanisms with which intrinsic properties would interact. Hence, the combination of spike frequency adaptation with synaptic depression in the network allows the computation of the rate of change of the stimulus (Puccini et al. 2007) and a higher detectability of unexpected stimulus (Puccini et al. 2006), a property described in the auditory cortex (Ulanovsky et al. 2003).

K^+ Current-Mediated Spike Frequency Adaptation in the Awake Animals

A similar time course of adaptation was found in this study between in vitro and in awake but the attenuation of the responses was larger in the awake animal (Fig. 3*D*). One possible factor contributing to this difference is the heterogeneity of neuronal classes recorded in the awake animal while in vitro only regular spiking neurons were included. Intrinsically bursting neurons recorded in vitro were not included given the difficulty to measure adaptation in a way comparable with that in regular spiking neurons. In any event, cortical intrinsically bursting neurons in rat sensorimotor cortex have been described to have as well sodium-dependent potassium currents contributing to their AHPs (Franceschetti et al. 2003).

Ongoing firing in the awake animal is probably responsible at least in part for the lesser adaptation observed in vitro than in the awake animal. Adaptation in vitro increased when neurons were not silent, but awake-like background firing was artificially induced (Fig. 7). Still, adaptation in vitro remained less than in the awake animal (Fig. 7*G*). These findings suggest that intrinsic properties could underlie at least part of the sound adaptation existing in awake animals for intervals between 50 ms and 2 s, while leaving room for additional mechanisms. Other adaptation features found in the awake state were also observed in slices. These were the dependence of response (R2) on the duration and intensity of the first stimulus and the increased delay of adapted responses.

There is an additional possible bias that should be considered when comparing populations of recorded neurons both in vivo and in vitro: while recordings in vitro were intracellular and thus they did not select neurons on the basis of activity, those in vivo were extracellular and thus biased toward spiking neurons (Shoham et al. 2006).

Potassium currents have been thoroughly studied in vitro, however, their role in the awake, functioning brain is not well known. Studies of ionic currents require the use of techniques that are not fully viable in the awake freely moving animal, where only relatively short intracellular recordings are possible (Lee et al. 2006). The study of ionic channels in vitro is based on the idea that those currents must exist in the brain tissue in situ. However, it is difficult to extrapolate the knowledge obtained from in vitro, or even from the anesthetized preparations, to the awake and functioning brain. Here, we have concentrated on the activation of potassium currents by spikes. But it should be taken into account that in vivo, in addition to the changes in conductance and membrane potential induced by potassium channels activation, there are conductance and membrane potential changes due to excitatory and inhibitory inputs to neurons. The last ones were not mimicked in our in vitro simulations of in vivo discharge patterns.

The ionic currents that we describe here in A1 slices must exist in the brain of the awake rat, given that both species and brain area were the same. Furthermore, the slices studied here were obtained from adult animals and recorded at 34–35 °C. Ongoing spontaneous activity was generally absent in our slices while we report an average of 5 Hz firing rate in awake animals (Supplementary Fig. S2). Ongoing activity in the awake may induce K^+ currents activation even in the absence of stimulation, thus neurons could have a basal "preadaptation." We show that even if a neuron in vitro is tonically firing at a similar rate to spontaneous activity in vivo (Figs 5*C* and 7*D*) an AHP and decreased excitability follow a spike discharge. And indeed, we found that neurons with spontaneous activity display larger adaptation than silent ones (Fig. 7*G*). Still, ionic currents may be up or down regulated in the awake brain. On the one hand, norepinephrine blocks both Ca^{2+} and Na^+-dependent K^+ currents (Foehring et al. 1989), while acetylcholine does the same on the Na^+-dependent K^+ current (Schwindt et al. 1989) hence they neuromodulate depending on the brain state.

K^+ currents in vivo could on the other hand be amplified in the network by reverberation in cortical circuits (Lorente de Nó 1949). In an active interconnected network, the decreased firing induced by K^+ currents is transmitted to connected neurons as decreased synaptic activity. The observation that Na^+ entering the cells through AMPA receptors is enough to activate Ca^{2+} and Na^+-dependent K^+ current (Nanou et al. 2008) would contribute to the even further amplification of its effect at the network level.

In conclusion, our results indicate that intrinsic properties of auditory cortical neurons probably participate as functional mechanisms mediating adaptation to sounds. The modulation of K^+ channels through adrenergic or cholinergic neurotransmitters (Foehring et al. 1989; Schwindt et al. 1989) could thus be a key mechanism in the top-down modulation of auditory adaptation through attention (Fritz et al. 2007).

Supplementary Material

Supplementary material can be found at: http://www.cercor.oxfordjournals.org/

Funding

Spanish Ministry of Science and Innovation (Spain) (BFU2008-01371/BFI); PRESENCCIA project (EU-FP6-27731).

Notes

We thank J. O'Keefe and collaborators from UCL for their generous help on the use of tetrodes, M. S. Malmierca (INCYL, University of Salamanca) and A. Zador (CSHL) for their suggestions regarding

auditory stimulation. The valuable contribution of D. Pérez-Marcos, L. Alonso, L. Pérez Méndez, and M. Pérez-Zabalza with respect to Matlab programming is acknowledged. We are grateful for the comments on the manuscript by M. S. Malmierca (INCYL, University of Salamanca), Lionel G. Nowak (University of Toulousse), and Peter S. Pennefather (University of Toronto). *Conflict of Interest*: None declared.

References

Aghajanian GK, Rasmussen K. 1989. Intracellular studies in the facial nucleus illustrating a simple new method for obtaining viable motoneurons in adult rat brain slices. Synapse. 3:331–338.

Anderson LA, Christianson GB, Linden JF. 2009. Stimulus-specific adaptation occurs in the auditory thalamus. J Neurosci. 29: 7359–7363.

Anderson SE, Kilgard MP, Sloan AM, Rennaker RL. 2006. Response to broadband repetitive stimuli in auditory cortex of the unanesthetized rat. Hear Res. 213:107–117.

Antunes F, Covey E, Malmierca S. 2010. Is there stimulus-specific adaptation in the auditory thalamus? The Neurophysiological Bases of Auditory Perception. New York: Springer. p. 535–544.

Bair W, Cavanaugh JR, Movshon JA. 2003. Time course and time-distance relationships for surround suppression in macaque V1 neurons. J Neurosci. 23:7690–7701.

Bartlett EL, Wang X. 2005. Long-lasting modulation by stimulus context in primate auditory cortex. J Neurophysiol. 94:83–104.

Bertorelli R, Ferri N, Adami M, Ongini E. 1996. Effects of four antiepileptic drugs on sleep and waking in the rat under both light and dark phases. Pharmacol Biochem Behav. 53:559–565.

Bhattacharjee A, Kaczmarek LK. 2005. For K+ channels, Na+ is the new Ca2+. Trends Neurosci. 28:422–428.

Brosch M, Schreiner CE. 1997. Time course of forward masking tuning curves in cat primary auditory cortex. J Neurophysiol. 77:923–943.

Buonomano DV, Merzenich MM. 1998. Net interaction between different forms of short-term synaptic plasticity and slow-IPSPs in the hippocampus and auditory cortex. J Neurophysiol. 80:1765–1774.

Calford MB, Semple MN. 1995. Monaural inhibition in cat auditory cortex. J Neurophysiol. 73:1876–1891.

Carandini M, Heeger DJ, Senn W. 2002. A synaptic explanation of suppression in visual cortex. J Neurosci. 22:10053–10065.

Chimoto S, Kitama T, Qin L, Sakayori S, Sato Y. 2002. Tonal response patterns of primary auditory cortex neurons in alert cats. Brain Res. 934:34–42.

Compte A, Sanchez-Vives MV, McCormick DA, Wang XJ. 2003. Cellular and network mechanisms of slow oscillatory activity (<1 Hz) and wave propagations in a cortical network model. J Neurophysiol. 89:2707–2725.

De Ribaupierre F, Goldstein MH, Jr., Yeni-Komshian G. 1972a. Cortical coding of repetitive acoustic pulses. Brain Res. 48:205–225.

De Ribaupierre F, Goldstein MH, Jr., Yeni-Komshian G. 1972b. Intracellular study of the cat's primary auditory cortex. Brain Res. 48:185–204.

Descalzo VF, Nowak LG, Brumberg JC, McCormick DA, Sanchez-Vives MV. 2005. Slow adaptation in fast spiking neurons of visual cortex. J Neurophysiol. 93:1111–1118.

Diaz-Quesada M, Maravall M. 2008. Intrinsic mechanisms for adaptive gain rescaling in barrel cortex. J Neurosci. 28:696–710.

Doron NN, Ledoux JE, Semple MN. 2002. Redefining the tonotopic core of rat auditory cortex: physiological evidence for a posterior field. J Comp Neurol. 453:345–360.

Eggermont JJ. 1999. The magnitude and phase of temporal modulation transfer functions in cat auditory cortex. J Neurosci. 19:2780–2788.

Eytan D, Brenner N, Marom S. 2003. Selective adaptation in networks of cortical neurons. J Neurosci. 23:9349–9356.

Fitzpatrick DC, Kuwada S, Kim DO, Parham K, Batra R. 1999. Responses of neurons to click-pairs as simulated echoes: auditory nerve to auditory cortex. J Acoust Soc Am. 106:3460–3472.

Foehring RC, Schwindt PC, Crill WE. 1989. Norepinephrine selectively reduces slow Ca2+- and Na+-mediated K+ currents in cat neocortical neurons. J Neurophysiol. 61:245–256.

Franken P, Tobler I, Borbely AA. 1995. Varying photoperiod in the laboratory rat: profound effect on 24-h sleep pattern but no effect on sleep homeostasis. Am J Physiol. 269:R691–701.

Fritz JB, Elhilali M, David SV, Shamma SA. 2007. Does attention play a role in dynamic receptive field adaptation to changing acoustic salience in A1? Hear Res. 229:186–203.

Gaese BH, Ostwald J. 2001. Anesthesia changes frequency tuning of neurons in the rat primary auditory cortex. J Neurophysiol. 86:1062–1066.

Gervasoni D, Lin SC, Ribeiro S, Soares ES, Pantoja J, Nicolelis MA. 2004. Global forebrain dynamics predict rat behavioral states and their transitions. J Neurosci. 24:11137–11147.

Hildebrandt KJ, Benda J, Hennig RM. 2009. The origin of adaptation in the auditory pathway of locusts is specific to cell type and function. J Neurosci. 29:2626–2636.

Hocherman S, Gilat E. 1981. Dependence of auditory cortex evoked unit activity on interstimulus interval in the cat. J Neurophysiol. 45:987–997.

Hromadka T, Deweese MR, Zador AM. 2008. Sparse representation of sounds in the unanesthetized auditory cortex. PLoS Biol. 6:e16.

Kilgard MP, Merzenich MM. 1999. Distributed representation of spectral and temporal information in rat primary auditory cortex. Hear Res. 134:16–28.

Koontz WLG, Fukunaga K. 1972. Asymptotic analysis of a nonparametric clustering technique. IEEE Trans Comput. 21:967–974.

Kuznetsova MS, Higgs MH, Spain WJ. 2008. Adaptation of firing rate and spike-timing precision in the avian cochlear nucleus. J Neurosci. 28:11906–11915.

Lee AK, Manns ID, Sakmann B, Brecht M. 2006. Whole-cell recordings in freely moving rats. Neuron. 51:399–407.

Lorente de Nó R. 1949. Cerebral cortex: architecture, intracortical connections, motor projections. In: Fulton JF, editor. Physiology of the nervous system. New York: Oxford University Press. p. 228–330.

Malmierca MS. 2003. The structure and physiology of the rat auditory system: an overview. Int Rev Neurobiol. 56:147–211.

Malmierca MS, Cristaudo S, Perez-Gonzalez D, Covey E. 2009. Stimulus-specific adaptation in the inferior colliculus of the anesthetized rat. J Neurosci. 29:5483–5493.

McCormick DA, Connors BW, Lighthall JW, Prince DA. 1985. Comparative electrophysiology of pyramidal and sparsely spiny stellate neurons of the neocortex. J Neurophysiol. 54:782–806.

Moshitch D, Las L, Ulanovsky N, Bar-Yosef O, Nelken I. 2006. Responses of neurons in primary auditory cortex (A1) to pure tones in the halothane-anesthetized cat. J Neurophysiol. 95:3756–3769.

Nanou E, Kyriakatos A, Bhattacharjee A, Kaczmarek LK, Paratcha G, El Manira A. 2008. Na+-mediated coupling between AMPA receptors and KNa channels shapes synaptic transmission. Proc Natl Acad Sci U S A. 105:20941–20946.

Nelken I, Fishbach A, Las L, Ulanovsky N, Farkas D. 2003. Primary auditory cortex of cats: feature detection or something else? Biol Cybern. 89:397–406.

Nowak LG, Azouz R, Sanchez-Vives MV, Gray CM, McCormick DA. 2003. Electrophysiological classes of cat primary visual cortical neurons in vivo as revealed by quantitative analyses. J Neurophysiol. 89:1541–1566.

Ojima H, Murakami K. 2002. Intracellular characterization of suppressive responses in supragranular pyramidal neurons of cat primary auditory cortex in vivo. Cereb Cortex. 12:1079–1091.

Oswald AM, Schiff ML, Reyes AD. 2006. Synaptic mechanisms underlying auditory processing. Curr Opin Neurobiol. 16:371–376.

Paxinos G, Watson C. 1998. The rat brain in stereotaxic coordinates. 4th ed. San Diego (CA): Academic Press.

Pennefather P, Lancaster B, Adams PR, Nicoll RA. 1985. Two distinct Ca-dependent K currents in bullfrog sympathetic ganglion cells. Proc Natl Acad Sci U S A. 82:3040–3044.

Percaccio CR, Engineer ND, Pruette AL, Pandya PK, Moucha R, Rathbun DL, Kilgard MP. 2005. Environmental enrichment increases paired-pulse depression in rat auditory cortex. J Neurophysiol. 94:3590–3600.

Perez-Gonzalez D, Malmierca MS, Covey E. 2005. Novelty detector neurons in the mammalian auditory midbrain. Eur J Neurosci. 22:2879–2885.

Pienkowski M, Eggermont JJ. 2009. Effects of adaptation on spectro-temporal receptive fields in primary auditory cortex. Neuroreport. 20:1198–1203.

Polley DB, Steinberg EE, Merzenich MM. 2006. Perceptual learning directs auditory cortical map reorganization through top-down influences. J Neurosci. 26:4970–4982.
Puccini GD, Sanchez-Vives MV, Compte A. 2006. Selective detection of abrupt input changes by integration of spike-frequency adaptation and synaptic depression in a computational network model. J Physiol Paris. 100:1–15.
Puccini GD, Sanchez-Vives MV, Compte A. 2007. Integrated mechanisms of anticipation and rate-of-change computations in cortical circuits. PLoS Comput Biol. 3:e82.
Qin L, Sato Y. 2004. Suppression of auditory cortical activities in awake cats by pure tone stimuli. Neurosci Lett. 365:190–194.
Read HL, Winer JA, Schreiner CE. 2002. Functional architecture of auditory cortex. Curr Opin Neurobiol. 12:433–440.
Reale RA, Brugge JF. 2000. Directional sensitivity of neurons in the primary auditory (AI) cortex of the cat to successive sounds ordered in time and space. J Neurophysiol. 84:435–450.
Reig R, Gallego R, Nowak LG, Sanchez-Vives MV. 2006. Impact of cortical network activity on short-term synaptic depression. Cereb Cortex. 16:688–695.
Rennaker RL, Carey HL, Anderson SE, Sloan AM, Kilgard MP. 2007. Anesthesia suppresses nonsynchronous responses to repetitive broadband stimuli. Neuroscience. 145:357–369.
Sah P. 1996. Ca(2+)-activated K+ currents in neurones: types, physiological roles and modulation. Trends Neurosci. 19:150–154.
Sakai M, Chimoto S, Qin L, Sato Y. 2009. Neural mechanisms of interstimulus interval-dependent responses in the primary auditory cortex of awake cats. BMC Neurosci. 10:10.
Sanchez-Vives MV, Nowak LG, McCormick DA. 2000a. Cellular mechanisms of long-lasting adaptation in visual cortical neurons in vitro. J Neurosci. 20:4286–4299.
Sanchez-Vives MV, Nowak LG, McCormick DA. 2000b. Membrane mechanisms underlying contrast adaptation in cat area 17 in vivo. J Neurosci. 20:4267–4285.
Schwindt PC, Spain WJ, Crill WE. 1989. Long-lasting reduction of excitability by a sodium-dependent potassium current in cat neocortical neurons. J Neurophysiol. 61:233–244.
Schwindt PC, Spain WJ, Foehring RC, Chubb MC, Crill WE. 1988. Slow conductances in neurons from cat sensorimotor cortex in vitro and their role in slow excitability changes. J Neurophysiol. 59:450–467.
Schwindt PC, Spain WJ, Foehring RC, Stafstrom CE, Chubb MC, Crill WE. 1988. Multiple potassium conductances and their functions in neurons from cat sensorimotor cortex in vitro. J Neurophysiol. 59:424–449.
Shoham S, O'Connor DH, Segev R. 2006. How silent is the brain: is there a "dark matter" problem in neuroscience? J Comp Physiol A Neuroethol Sens Neural Behav Physiol. 192:777–784.
Stephenson R, Caron AM, Cassel DB, Kostela JC. 2009. Automated analysis of sleep-wake state in rats. J Neurosci Methods. 184:263–274.
Szymanski F, Garcia-Lazaro J, Schnupp JW. 2009. Current source density profiles of stimulus-specific adaptation in rat auditory cortex. J Neurophysiol. 102:1483–1490.
Tan AY, Zhang LI, Merzenich MM, Schreiner CE. 2004. Tone-evoked excitatory and inhibitory synaptic conductances of primary auditory cortex neurons. J Neurophysiol. 92:630–643.
Ter-Mikaelian M, Sanes DH, Semple MN. 2007. Transformation of temporal properties between auditory midbrain and cortex in the awake Mongolian gerbil. J Neurosci. 27:6091–6102.
Uchimura N, Cherubini E, North RA. 1990. Cation current activated by hyperpolarization in a subset of rat nucleus accumbens neurons. J Neurophysiol. 64:1847–1850.
Ulanovsky N, Las L, Farkas D, Nelken I. 2004. Multiple time scales of adaptation in auditory cortex neurons. J Neurosci. 24:10440–10453.
Ulanovsky N, Las L, Nelken I. 2003. Processing of low-probability sounds by cortical neurons. Nat Neurosci. 6:391–398.
Varela JA, Sen K, Gibson J, Fost J, Abbott LF, Nelson SB. 1997. A quantitative description of short-term plasticity at excitatory synapses in layer 2/3 of rat primary visual cortex. J Neurosci. 17:7926–7940.
Vergara C, Latorre R, Marrion NV, Adelman JP. 1998. Calcium-activated potassium channels. Curr Opin Neurobiol. 8:321–329.
Volkov IO, Galazjuk AV. 1991. Formation of spike response to sound tones in cat auditory cortex neurons: interaction of excitatory and inhibitory effects. Neuroscience. 43:307–321.
von der Behrens W, Bauerle P, Kossl M, Gaese BH. 2009. Correlating stimulus-specific adaptation of cortical neurons and local field potentials in the awake rat. J Neurosci. 29:13837–13849.
Wehr M, Zador AM. 2005. Synaptic mechanisms of forward suppression in rat auditory cortex. Neuron. 47:437–445.
Werner-Reiss U, Porter KK, Underhill AM, Groh JM. 2006. Long lasting attenuation by prior sounds in auditory cortex of awake primates. Exp Brain Res. 168:272–276.
Zhang LI, Tan AY, Schreiner CE, Merzenich MM. 2003. Topography and synaptic shaping of direction selectivity in primary auditory cortex. Nature. 424:201–205.